Inorg. Chem. **2004**, *43*, 3871–3881

Rotational Spectra, Structures, Hyperfine Constants, and the Nature of the Bonding of KrCuF and KrCuCl

Julie M. Michaud, Stephen A. Cooke, and Michael C. L. Gerry*

Department of Chemistry, The University of British Columbia, 2036 Main Mall, Vancouver, B.C., Canada V6T 1Z1

Received January 23, 2004

Rotational spectra of KrCuF and KrCuCl have been measured in the frequency range 8–18 GHz, using a pulsed jet cavity Fourier transform microwave spectrometer. The molecules were prepared by ablating Cu metal with a pulsed Nd:YAG laser (1064 nm) and allowing the plasma to react with appropriate precursors (Kr plus SF_6 or Cl_2) contained in the backing gas of the jet (Ar or Kr). Rotational constants, internuclear distances, vibration frequencies, and ^{83}Kr, Cu, and Cl nuclear quadrupole coupling constants have all been evaluated. The Kr–Cu bonds are short and the complexes are rigid. The ^{83}Kr coupling constant of KrCuF is large (128.8 MHz). The Cu nuclear quadrupole coupling constants differ radically from those of uncomplexed CuF and CuCl molecules. The results are supported by those of ab initio calculations, which have also yielded Mulliken populations, MOLDEN plots of valence molecular orbitals and Laplace concentrations, and electron localization functions. The results are consistent with those reported earlier for other noble gas–noble metal halide complexes. The results have been used to assess the nature of the bonding in the complexes and have produced good evidence for weak noble gas–noble metal chemical bonding.

Introduction

Recently, we have reported the microwave spectra and geometries of a series of linear complexes with the general formula NgMX (Ng = Ar, Kr, Xe; M = Cu, Ag, Au; X = F, Cl, Br).[1−8] An example is KrAgCl.[5] The Ng−M bonds are unexpectedly short, ranging in length from 2.22−2.30 Å for Ar−Cu,[2] through 2.39−2.52 Å for Ar−Au and Kr−Au,[3,4,7] to 2.56−2.66 Å for Ar−Ag and Kr−Ag.[1,5−7] These are much less than the lengths usually found for Ng−neutral molecule van der Waals complexes, though r(Ar−Na) = 2.889 Å in the van der Waals complex Ar−NaCl.[9] The centrifugal distortion constants, D_J, evaluated from the spectra, are all less than 1 kHz, indicating the complexes to be rather rigid. This is in contrast to 9 kHz found for the much more flexible Ar−NaCl.[9] The NgMX complexes are apparently rather strongly bound.

The results are supported by those from MP2 ab initio calculations.[1−8,10] The bond lengths are reproduced. Stretching frequencies ω(Ng−M) agree with those calculated from D_J. In addition, MOLDEN plots of occupied valence molecular orbitals are consistent with electron sharing between the noble gas and metal. Mulliken populations suggest the donation of up to 0.2 electron from Ng to M. Plots of Laplace concentrations indicate possible small electron density buildup between Ng and M. The possibility of weak Ng−M chemical bonding is implied.

This suggestion is supported by the nuclear quadrupole coupling constants of all three atoms. For both M and X, large changes are found in their eQq values when Ar or Kr attaches to MX.[1−7] These changes are ∼35−40% of those found when MX is converted to XMX^- ions (e.g., $BrAuBr^-$); these ions are isoelectronic with the NgMX complexes. Such

* Author to whom correspondence should be addressed. E-mail: mgerry@chem.ubc.ca.

(1) Evans, C. J.; Gerry, M. C. L. *J. Chem. Phys.* **2000**, *112*, 1321.
(2) Evans, C. J.; Gerry, M. C. L. *J. Chem. Phys.* **2000**, *112*, 9363.
(3) Evans, C. J.; Lesarri, A.; Gerry, M. C. L. *J. Am. Chem. Soc.* **2000**, *122*, 6100.
(4) Evans, C. J.; Rubinoff, D. S.; Gerry, M. C. L. *Phys. Chem. Chem. Phys.* **2000**, *2*, 3943.
(5) Reynard, L. M.; Evans. C. J.; Gerry, M. C. L. *J. Mol. Spectrosc.* **2001**, *206*, 33.
(6) Walker, N. R.; Reynard, L. M.; Gerry, M. C. L. *J. Mol. Struct.* **2002**, *612*, 109.
(7) Thomas, J. M.; Walker, N. R.; Cooke, S. A.; Gerry, M. C. L. *J. Am. Chem. Soc.* **2004**, *126*, 1235.
(8) Cooke, S. A.; Gerry, M. C. L. *Phys. Chem. Chem. Phys.* **2004**, published on the web, May 17, 2004.
(9) Mizoguchi, A.; Endo, Y.; Ohshima, Y. *J. Chem. Phys.* **1998**, *109*, 10539.
(10) Lovallo, C. C.; Klobukowski, M. *Chem. Phys. Lett.* **2002**, *368*, 589.

10.1021/ic040009s CCC: $27.50
Published on Web 05/27/2004

changes indicate a significant reorganization of the MX electron distribution on complex formation.

The quadrupole coupling data are even more dramatic for the Ng atom. Nuclear quadrupole coupling constants (NQCCs) for both ^{83}Kr and ^{131}Xe have been reported.[7,8] The trends for both Kr and Xe are similar. For ^{83}Kr, for example, whereas $eQq = 0$ for the isolated atom, values of ~105 and ~186 MHz have been found for ^{83}KrAgF and ^{83}KrAuF, respectively. These are in contrast to ~5 MHz for ^{83}Kr−HCl, a typical atom−neutral molecule van der Waals complex.[11] These results are clearly consistent with unusually strong bonding in noble gas−noble metal halide complexes and support the possibility of weak Ng−M chemical bonding.

Support for such a view also comes from data on the NgM^+ ions. In a recent review,[12] Bellert and Breckenridge could rationalize their bonding in terms of electrostatics for all metals, M, except for some complexes of noble metals. $XeAu^+$ seems especially anomalous, with $KrAu^+$ and $ArAu^+$ being less so. They felt that $NgAg^+$ and $NgCu^+$ fit the usual pattern. These results have been considered in our recent reassessment of the nature of the NgMX bonding,[7] where it is concluded that chemical bonding is likely in NgAuX and possible in NgCuX and NgAgX.

Although spectra of 15 NgMX complexes have been reported, only three of these have contained Cu, and all three were ArCuX.[2] Yet spectra of others are needed to reveal a complete picture of the bonding. The Ar−Cu bonds are the shortest so far reported, but their bond energies are apparently intermediate between those of the Ar−Ag and Ar−Au bonds. Spectra of further complexes, containing Kr and Xe, would be of interest, not just to fill in the data set. Hyperfine coupling for both nuclei should provide excellent information on the electron distribution of the molecule. Spectra of KrCuX and XeCuX were not anticipated to be easy to observe because of the multitude of possible isotopic species, all producing greater or lesser hyperfine structure. However, it has now been possible to measure spectra of both KrCuF and KrCuCl, including ^{83}Kr^{63}CuF. These results and their implications are reported in this paper.

Experimental Methods

The spectra were measured with a Balle−Flygare-type[13] cavity pulsed jet Fourier transform microwave (FTMW) spectrometer; it has been described in detail earlier.[14] The cell is a Fabry−Perot cavity, containing two spherical aluminum mirrors 28.5 cm in diameter, with a radius of curvature of 38 cm, held approximately 30 cm apart. The cavity is frequency-tuned by moving one of the mirrors; the other mirror is held fixed in place. Samples are injected entrained in a noble gas from a pulsed nozzle (General Valve Series 9), mounted in the fixed mirror. Although this arrangement optimizes both the sensitivity and resolution of the spectrometer, each line is doubled by the Doppler effect.

The complexes were produced in the laser ablation source, whose design has been given earlier.[15] A 5 mm diameter Cu rod mounted in front of the nozzle was ablated with the fundamental (1064 nm) of a pulsed Nd:YAG laser. The rod was rotated and translated to provide a fresh surface for each laser pulse. The Cu plasma reacted with a precursor gas contained in the backing gas of the jet, and the reaction products were injected into the cell. To prepare KrCuF, ~0.5% SF_6 in pure Kr was used; to prepare KrCuCl, ~0.5% Cl_2 in 33% Kr in Ar was used. The backing pressures were 6−7 atm.

The concentrations and lifetimes of the samples vary with backing gas composition. Accordingly, the timings of the laser, microwave, and sample pulses had to be varied to optimize the signal-to-noise ratios of each sample. The most intense spectra were obtained with microwave pulse lengths of 0.2 μs, the shortest available with our spectrometer, consistent with high dipole moments for the sample molecules. Though the strongest lines of KrCuF could be seen clearly with ~60 pulses, the lines of samples containing ^{83}Kr, namely ^{83}Kr^{63}Cu^{19}F, required ~20 000 pulses for a good signal-to-noise ratio.

The spectra were observed in the frequency range 8−18 GHz. Line frequency measurements were referenced to a Loran frequency standard, accurate to 1 part in 10^{10}. The observed line widths were ~7−10 kHz (fwhm), and the reported line frequencies have an estimated accuracy of ±1 kHz.

Quantum Chemical Calculations. Ab initio calculations were performed at the second-order Møller−Plesset (MP2) level of theory, using the GAUSSIAN 98 suite of programs.[16] For F and Kr, we used the simple 6-31G(d) basis set and the cc-pVTZ basis set, [17] respectively. For Cl, we used the (631111s/52111p) McLean−Chandler basis set,[18] augmented with one d-polarization function ($\alpha_d = 0.75$).[19] For Cu, an effective core potential (ECP) was used, which left 19 valence electrons ($3s^2 3p^6 3d^{10} 4s^1$). The ECP for Cu and the optimized Gaussian basis set (31111s/22111p/411d) were taken from Andrae et al.[20] The Cu basis set was further augmented with two f-functions, $\alpha_f = 3.1235$ and $\alpha_f = 1.3375$.[19] In the calculation of dissociation energies, the counterpoise correction was applied to account for basis set superposition error (BSSE).[21] All structures were constrained to a linear geometry.

Spectra and Analysis. (i) KrCuF. A preliminary rotational constant of the most abundant isotopomer, ^{84}Kr^{63}Cu^{19}F, was estimated using the ab initio bond lengths of Lovallo and Klobukowski.[10] It, along with the ^{63}Cu nuclear quadrupole coupling constant, eQq (^{63}Cu), of ArCuF,[2] was used in a prediction of the spectrum. The first searches were near 8640 MHz, for the $J = 4-3$ transition.

(11) Campbell, E. J.; Buxton, L. W.; Keenan, M. R.; Flygare, W. H. *Phys. Rev. A: At., Mol., Opt. Phys.* **1981**, *24*, 812.
(12) Bellert, D.; Breckenridge, W. H. *Chem. Rev.* **2002**, *102*, 1595.
(13) Balle, T. J.; Flygare, W. H. *Rev. Sci. Instrum.* **1989**, *52*, 33.
(14) Xu, Y.; Jäger, W.; Gerry, M. C. L. *J. Mol. Spectrosc.* **1992**, *151*, 206.
(15) Walker, K. A.; Gerry, M. C. L. *J. Mol. Spectrosc.* **1997**, *182*, 178.
(16) Frisch, M. J.; Trucks, G. W.; Schlegel, H. B.; Scuseria, G. E.; Robb, M. A.; Cheeseman, J. R.; Zakrzewski, V. G.; Montgomery, J. A.; Stratmann, R. E.; Burant, J. C.; Dapprich, S.; Milliam, J. M.; Daniels, A. D.; Rudin, K. N.; Strain, M. C.; Farkas, O.; Tomasi, J.; Barone, V.; Cossi, M.; Cammi, R.; Mennucci, B.; Pomelli, C.; Adamo, C.; Clifford, S.; Ochterski, J.; Peterson, G. A.; Ayala, P. Y.; Cui, Q.; Morokuma, K.; Malick, D. K.; Rabuck, A. D.; Raghavachari, K.; Foresman, J. B.; Cioslowski, J.; Ortiz, J. V.; Stefanov, B. B.; Liu, G.; Liashenko, A.; Piskorz, P.; Komaroni, I.; Gomperts, R.; Martin, R. L.; Fox, D. J.; Keith, T.; Al-Lahma, M. A.; Peng, C. Y.; Nanayakkara, A.; Gonzalez, C.; Challacombe, M.; Gill, P. M. W.; Johnson, B. G.; Chen, W.; Wong, M. W.; Andres, J. L.; Head-Gordon, M.; Replogle, E. S.; Pople, J. A. *Gaussian 98*, revision A.6; Gaussian Inc.: Pittsburgh PA, 1998.
(17) (a) Woon, D. E.; Dunning, T. H., Jr. *J. Chem. Phys.* **1993**, *98*, 1358. (b) Wilson, A. K.; Woon, D. E.; Peterson, K. A.; Dunning, T. H., Jr. *J. Chem. Phys.* **1999**, *110*, 7667.
(18) McLean, A. D.; Chandler, G. S. *J. Chem. Phys.* **1980**, *72*, 5639.
(19) Antes, I.; Dapprich, S.; Frenking, G.; Schwerdtfeger, P. *Inorg. Chem.* **1996**, *35*, 2089.
(20) Andrae, D.; Häusermann, V.; Dolg, M.; Stoll, H.; Preus, H. *Theor. Chim. Acta* **1990**, *27*, 213.
(21) Hobza, P.; Zahraduik, R. *Chem. Rev.* **1988**, *88*, 871.

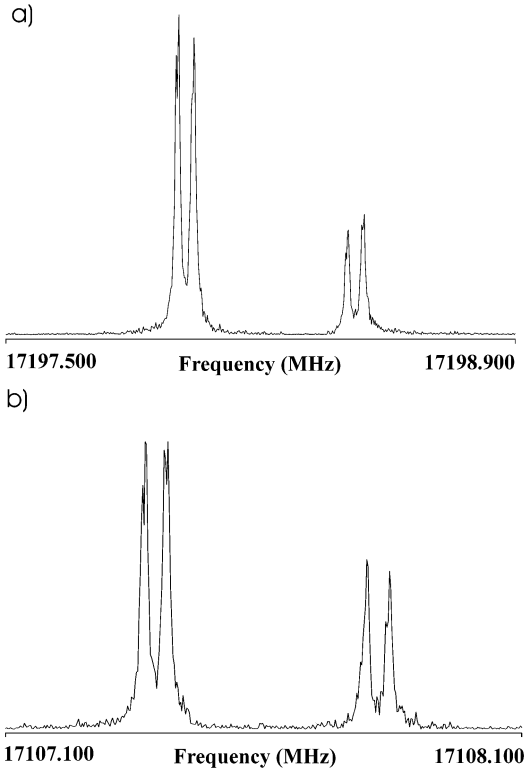

Figure 1. Portions of the observed hyperfine structures in the $J = 6-5$ transitions of (a) $^{84}Kr^{63}CuF$ and (b) $^{84}Kr^{65}CuF$. In both cases, 1000 averaging cycles were taken over 4k data points; an 8k transform was used.

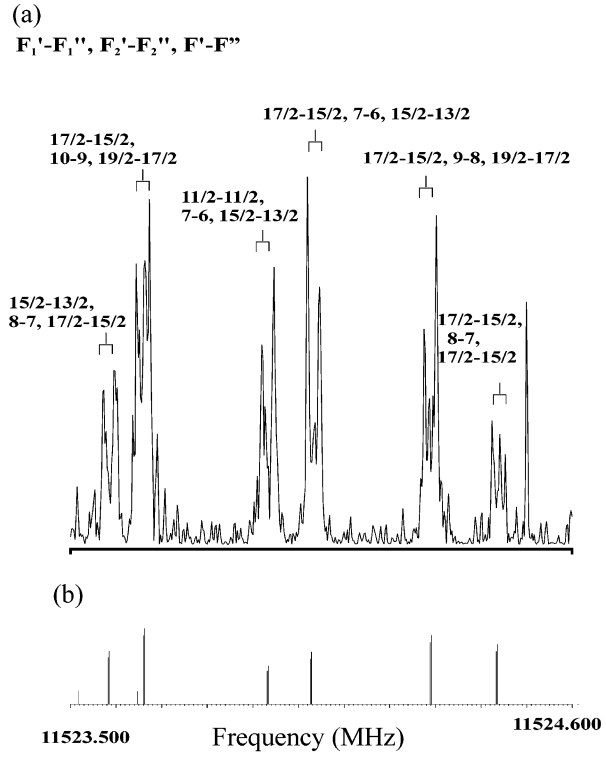

Figure 2. A portion of the hyperfine structure of the $J = 4-3$ transition of $^{83}Kr^{63}CuF$, compared with the pattern predicted with the derived hyperfine coupling constants. In the experimental spectrum, 20 000 averaging cycles were taken over 4k data points; an 8k transform was used.

The first peaks, found near 8690 MHz, were somewhat weaker than expected; they were accordingly assigned to a minor isotopomer, and the searches continued. A much stronger group, found near 8590 MHz, was assigned to $^{84}Kr^{63}Cu^{19}F$. These signals disappeared when laser ablation was omitted, or when SF_6 was omitted from the preparation mixture. Furthermore, successive $(J+1)-J$ transitions, separated by $2B_o$, were found, as expected for a linear molecule.

The assignments were confirmed further by the isotopic dependences of the spectra. The relative frequencies of the different isotopomers could be predicted from the atomic masses and the geometry. The intensities were consistent with the relative isotopic abundances. Each transition showed hyperfine structure due to Cu nuclear quadrupole coupling; the ratios of the ^{63}Cu and ^{65}Cu nuclear quadrupole coupling constants (from the fits described below) for corresponding isotopomers followed the ratio of the quadrupole moments. Some transitions showed small but measurable further splittings due to ^{19}F spin−rotation coupling. Finally, the transitions of $^{83}Kr^{63}Cu^{19}F$ showed further hyperfine structure due to nuclear quadrupole coupling of ^{83}Kr($I = 9/2$). Some example transitions are shown in Figures 1 and 2.

The measured frequencies are given with their quantum number assignments in the Supporting Information. For all isotopic species except $^{83}Kr^{63}Cu^{19}F$, the quantum number assignments follow the coupling scheme $\mathbf{J} + \mathbf{I}_{Cu} = \mathbf{F_1}$; $\mathbf{F_1} + \mathbf{I}_F = \mathbf{F}$. The spectra were analyzed using Pickett's global least-squares fitting program SPFIT.[22] Each isotopic species was treated separately.

To obtain a good fit for $^{84}Kr^{63}Cu^{19}F$, nuclear spin−rotation constants for both ^{63}Cu and ^{19}F were included (C_l(Cu) and C_l(F)), along with a spin−spin coupling term for these two nuclei (α_{CuF}). There was only a marginal difference in the fit, depending on whether α_{CuF} was a scalar or a tensor constant; the latter gave a slightly better fit and was retained. It should be noted that there was nothing in the appearance of the spectrum to confirm the quantum number assignments of these very small splittings. The sign of α_{CuF} depended on the choice made. Given that both Cu and F are nearer the top than the bottom of the periodic table, the sign of α_{CuF} was chosen as that for direct coupling, and assignments followed accordingly. The choice made no difference to the structural conclusions given below. It is fair to say that α_{CuF}, probably C_l(F), and possibly C_l(Cu) are best regarded as simply fitting parameters. Fits to the remaining isotopomers also included these constants, though in most cases, one or more were held fixed. This is indicated in Table 1, which presents all the derived spectroscopic constants for this complex.

The transitions of $^{83}Kr^{63}Cu^{19}F$ were much weaker and more complex because of the additional ^{83}Kr hyperfine splittings. Prediction of the rotational constant was straightforward, either by interpolation between those of other isotopomers or by using the geometry derived from them. Prediction of the hyperfine patterns was less simple. The method chosen was to fix $eQq(^{63}Cu)$ at its value for other isotopomers, and then to predict a series of line patterns with $eQq(^{83}Kr)$ intermediate between those of KrAgF and KrAuF. This led to an excellent match, part of which is shown in Figure 2. From this, quantum number assignments were made according to the coupling scheme $\mathbf{J} + \mathbf{I}_{Kr} = \mathbf{F_1}$; $\mathbf{F_1} + \mathbf{I}_{Cu} = \mathbf{F_2}$; $\mathbf{F_2} + \mathbf{I}_F = \mathbf{F}$. A fit of the spectra using this scheme in SPFIT[22] produced the spectroscopic constants for this isotopomer in Table 1.

(ii) KrCuCl. The predicted bond lengths of KrCuCl in ref 10 were scaled using the ratios of experimental and predicted bond lengths for KrCuF. Rotational constants calculated from these bond lengths guided initial spectral searches. The first groups, found near 7646 MHz, were again somewhat weaker than expected and assigned to a minor isotopomer. The strongest group in the vicinity,

(22) Pickett, H. M. *J. Mol. Spectrosc.* **1991**, *148*, 371.

Table 1. Spectroscopic Constants of KrCuF

parameter	$^{82}Kr^{63}CuF$	$^{82}Kr^{65}CuF$	$^{83}Kr^{63}CuF$	$^{84}Kr^{63}CuF$	$^{84}Kr^{65}CuF$	$^{86}Kr^{63}CuF$	$^{86}Kr^{65}CuF$
B_o (MHz)	1448.2467(2)[a]	1440.7921(2)	1440.6303(5)	1433.2064(1)	1425.6545(3)	1418.8143(2)	1411.1676(4)
D_J (kHz)	0.3862(33)	0.3371(35)	0.389(10)	0.3802(26)	0.3727(53)	0.3664(33)	0.3636(73)
eQq(Cu) (MHz)	41.79(3)	38.32(4)	41.51(5)	41.77(3)	38.654(5)	41.80(35)	38.63(10)
eQq(^{83}Kr) (MHz)			128.79(12)				
C_lCu) (kHz)	5.40[b]	5.68[c]	5.40[b]	5.40(17)	4.97(34)	5.40[b]	5.68[c]
C_l(F) (kHz)	5.82[b]	5.82[b]	5.82[b]	5.82(147)	5.82[b]	5.82[b]	5.82[b]
α_{CuF} (kHz)	3.58[b]	3.83[c]	3.58[b]	3.58(51)	3.83[c]	3.58[b]	3.83[c]

[a] Numbers in parentheses are one standard deviation in units of the last significant figure. [b] Fixed at the value for $^{84}Kr^{63}CuF$. [c] Fixed at the value for $^{84}Kr^{63}CuF$, scaled by the ratio of the ^{65}Cu and ^{63}Cu magnetic moments.

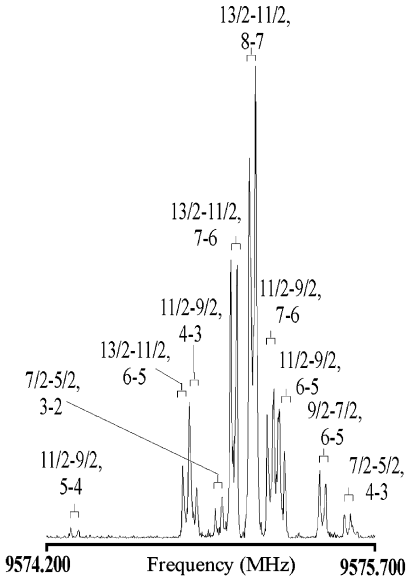

Figure 3. A portion of the hyperfine structure of the $J = 4-3$ transition of $^{84}Kr^{63}Cu^{35}Cl$. The experiment required 3700 averaging cycles taken over 4k data points; an 8k transform was used.

Table 2. Spectroscopic Constants of KrCuCl

isotopomer	B_o (MHz)	D_J (kHz)	eQq(Cu) (MHz)	eQq(Cl) (MHz)
$^{84}Kr^{63}Cu^{35}Cl$	957.5262(2)[a]	0.1489(24)	36.522(36)	−27.297(27)
$^{84}Kr^{65}Cu^{35}Cl$	955.8138(3)	0.1179(76)	32.930(80)	−27.153(61)
$^{86}Kr^{63}Cu^{35}Cl$	947.679(3)	0.143(9)	36.0(12)	−27.3(10)
$^{84}Kr^{63}Cu^{37}Cl$	931.2194(4)	0.1337(89)	36.41(11)	−21.533(39)

[a] Numbers in parentheses are one standard deviation in units of the last significant figure.

near 7660 MHz, was assigned to $J = 4-3$ of $^{84}Kr^{63}Cu^{35}Cl$. After optimum conditions to produce the spectra had been found, transitions of two further minor isotopomers were easily located. Three $(J+1)-J$ transitions were found for $^{84}Kr^{63}Cu^{35}Cl$, with two each for the remainder. The lines of $^{86}Kr^{63}Cu^{35}Cl$ were weak. All observed transitions showed nuclear quadrupole coupling due to both Cu and Cl; the quantum number assignments followed the scheme $\mathbf{J} + \mathbf{I}_{Cu} = \mathbf{F_1}$; $\mathbf{F_1} + \mathbf{I}_{Cl} = \mathbf{F}$. The same checks of the assignments as for those of KrCuF were carried out. Spectra of ^{83}KrCuCl were too weak to be observed.

The frequencies of all measured transitions are given with their quantum number assignments in the Supporting Information. A representative transition is depicted in Figure 3. The spectra were analyzed using SPFIT to give the spectroscopic constants in Table 2.

Structures of the Complexes. The rotational constants shown in Tables 1 and 2 have been used to determine the geometries of the complexes. Since the spectra are consistent with linear structures for both complexes, the parameters to be determined were the Kr−Cu and Cu−F (or Cu−Cl) internuclear distances. Ideally, the equilibrium (r_e) bond lengths should be obtained. However, since the complexes were observed only in their ground states, only approximate r_e values at best were available. The following procedures were used.

Table 3. Geometry[a] of KrCuF

method	r (Kr−Cu)	r (Cu−F)	comments
r_o	2.31801(61)[b]	1.7536(13)	
$r_{I\epsilon}$	2.318301(40)	1.74883(17)	$\epsilon = 0.431(14)$ uÅ^2
$r_m^{(1)}$	2.316887(52)	1.74777(20)	$c = 0.0459(14)$ u$^{1/2}$Å
$r_m^{(2)}$	2.31625(6)	1.744923[c]	$c = 0.097(3)$ u$^{1/2}$Å; $d = -0.108(8)$ u$^{1/2}$Å^2
MP2	2.28	1.73	
MP2[d]	2.322	1.730	

[a] Bond distances in Å. [b] Numbers in parentheses are one standard deviation in units of the last significant figure. [c] In the $r_m^{(2)}$ geometry, the CuF internuclear distance was fixed at r_e of CuF.[26] [d] Values predicted in ref 10.

An initial fit was made to the moments of inertia (I_o) corresponding to the ground-state rotational constants, B_o, using rigid rotor formulas and assuming no dependence of the structure on isotopomer or vibrations:

$$I_o = I_{rigid}(r_o) \tag{1}$$

This gave ground-state effective (r_o) bond lengths.

The vibrational dependence of the rotational constants can be accounted for, at least partially, by including an additional constant parameter, designated ϵ, assumed to be independent of isotopomer:

$$I_o = I_{rigid}(r_{I\epsilon}) + \epsilon \tag{2}$$

A fit to the bond lengths plus ϵ gave $r_{I\epsilon}$ values.[23] These are equivalent to the earlier substitution (r_s) bond lengths[24] when a large number of isotopomers is used.

Finally, the dependence of ϵ on the isotopomers was accounted for using the mass-dependent (r_m) structures of Watson et al.[25] For a linear triatomic molecule the equation is:

$$I_o = I_m + c(I_m)^{1/2} + d\left(\frac{m_1 m_2 m_3}{M}\right)^{1/4} \tag{3}$$

where $I_m = I_{rigid}(r_m)$, and c and d are constants; m_1, m_2, and m_3 are the atomic masses, and M is the molecular mass. A fit including c but omitting d produced an $r_m^{(1)}$ structure; a fit including both c and d gave an $r_m^{(2)}$ geometry.

The derived bond lengths of KrCuF are in Table 3. The r_o, $r_{I\epsilon}$, and $r_m^{(1)}$ parameters seem well-determined, with the r_o values being an order of magnitude less well-determined than the others,

(23) Rudolph, H. D. *Struct. Chem.* **1991**, *2*, 581.
(24) Costain, C. C. *J. Chem. Phys.* **1958**, *29*, 864.
(25) Watson, J. K. G.; Roytburg, A.; Ulrich, W. *J. Mol. Spectrosc.* **1999**, *196*, 202.

Table 4. Geometry[a] of KrCuCl

method	r (Kr−Cu)	r (Cu−Cl)	comments
r_o	2.36286(84)[b]	2.0525(12)	
$r_{I\epsilon}$	2.3592(23)	2.0538(12)	$\epsilon = 0.77(46)$ uÅ^2
$r_m^{(1)}$	2.357484(33)	2.05230(89)	$c = 0.067(40)$ u$^{1/2}$Å
$r_m^{(2)c}$	2.3563	2.05147	$c = 0.144$ u$^{1/2}$Å; $d = -0.224$ u$^{1/2}$Å^2
MP2	2.314	2.0415	
MP2[d]	2.369	2.055	
r_e(CuCl)[e]		2.051177[e]	

[a] Bond distances in Å. [b] Numbers in parentheses are one standard deviation in units of the last significant figure. [c] Exact calculation: four structural parameters from four rotational constants. [d] Reference 10. [e] Reference 27.

presumably because of isotopic variations in the ground-state bond lengths. An unconstrained $r_m^{(2)}$ fit produced highly correlated, poorly determined values probably because no isotopic substitution at F was possible. Accordingly, a fit with r(CuF), constrained to the value of r_e for CuF monomer,[26] was carried out. This was satisfactory and produced the values in Table 3. This table also presents the ab initio MP2 values from both this work and that in ref 10. They are in moderate agreement with experiment, though they agree poorly between themselves.

In one sense, KrCuCl was easier to deal with because isotopic substitutions could be made at all atoms, and there are no large correlations between the bond lengths. Again, reasonable values could be obtained using unconstrained fits to r_o, $r_{I\epsilon}$, and $r_m^{(1)}$ parameters, though the $r_{I\epsilon}$ fits seem poorer than the others. Since the $r_m^{(2)}$ calculations involved obtaining four parameters from four rotational constants, an exact calculation was carried out; it too gave reasonable values. All the derived bond lengths, plus those of the MP2 calculations, are in Table 4. The ab initio MP2 values from ref 10 agree well with experiment, but our values agree to a lesser extent.

Discussion

Molecular Structures. The newly determined Kr−Cu bond lengths are presented in Table 5, in comparison with the NgM bond lengths of all NgMX complexes reported to date, plus some related complexes. The ab initio values are also given.

From this table it is clear that the Kr−Cu bond lengths are consistent with those of the other NgMX complexes. The experimental values are slightly greater than the ab initio values. The Kr−Cu bonds are slightly longer than the Ar−Cu bonds, and the variations follow the trends predicted ab initio, not only for NgCuX but also for the $NgCuNg^+$ ions. The Kr−CuX bonds are significantly shorter than the Kr−AuX and Kr−AgX bonds for the same X (F, Cl, or Br), with similar trends predicted for $KrCuKr^+$ and $KrAuKr^+$.

Table 6 contains a comparison of the experimental Ng−M bond lengths with values obtained from two sums of standard parameters. One is the sum of the noble gas van der Waals radius and the M^+ ionic radius; this is effectively the van der Waals limit. The second is the sum of noble gas and M(I) radii, in what can be regarded as the covalent limit. The table is an extension of Table 11 in ref 7, modified slightly to reveal some clear trends which are beginning to emerge.

Table 5. Ng−M Bond Lengths (r), Centrifugal Distortion Constants (D_J), Stretching Frequencies (ω), Force Constants (k), and Calculated Dissociation Energies (D_e) of Noble Gas−Noble Metal Halides and Related Complexes

complex	r(NgM) (Å)	D_J (kHz)	ω(NgM) (cm^{-1})	ω(MX) (cm^{-1})	k(NgM) (N m^{-1})[d]	D_e (kJ mol^{-1})
	e (a)[a]	$\times 10^2$	e (a)[b]	c (m)[c]		c (u)[e]
ArCuF[f]	2.22 (2.19)	94	224 (228)	674 (621[g])	79	44, 37[h] (47)
ArCuCl[f]	2.27 (2.24)	34	197 (190)	456 (418[i])	65	33, 28[h] (37)
ArCuBr[f]	2.30 (2.26)	12	170 (164)	350 (313[j])	53	
$ArCuAr^{+}$[k]	(2.34)					(41)
KrCuF[l]	2.32 (2.28)	38	185 (198)	669 (621[g])	84	45, 48[h] (61)
KrCuCl[l]	2.36 (2.31)	15	162 (148)	441 (418[i])	70	37, 39[h] (53)
$KrCuKr^{+}$[k]	(2.42)					(58)
ArAgF[m]	2.56 (2.56)	95	141 (127)	541 (513[n])	36	14, 18[h] (17)
ArAgCl[m]	2.61 (2.59)	35	135 (120)	357 (344[o])	34	16, 16[h] (14)
ArAgBr[m]	2.64	11	124	(251[p])	30	
KrAgF[q]	2.59 (2.60)	31	125 (113)	544 (513[n])	48	17, 28[h] (32)
KrAgCl[r]	2.64 (2.63)	13	117 (105)	352 (344[o])	43	15, 26[h] (28)
KrAgBr[s]	2.66 (2.69)	4	106 (89)	255 (247[p])	38	17 (25)
XeAgF[t]	2.65 (2.74)	14	130 (108)	546(513[m])	64	36, 43[h] (56)
XeAgCl[t]	2.70(2.78)	6	120 (99)	356 (344[o])	58	33, 39[h] (54)
ArAuF[u]	2.39 (2.39)	51	221 (214)	583 (544[v])	97	55, 50[h] (59)
ArAuCl[w]	2.47 (2.46)	21	198 (184)	413 (383[x])	78	42, 38[h] (47)
ArAuBr[u]	2.50 (2.49)	6	178 (165)	286 (264[x])	65	
$ArAuAr^{+}$[y]	(2.54)		(141, 201)[y]			(44)
KrAuF[s]	2.46 (2.45)	16	176 (184)	(544[v])	110	58, 71[h] (86)
KrAuCl[w]	2.52 (2.51)	8	161 (163)	409 (383[x])	94	44, 56[h] (72)
$KrAuKr^{+}$[y]	(2.57)		(126, 186)[y]			(69)
Ar−NaCl[z]	2.89	900	21		0.6	(8)
ArHg[aa]	4.05		22			

[a] e = results of experiment. a = values calculated ab initio. [b] e = experimental values which for the NgMX complexes have been derived from the centrifugal distortion constants using a diatomic approximation. a = ab initio values. [c] c = ab initio values for the complex. m = experimental values for the monomer. [d] Force constant, k, derived from ω(Ng−M), using a diatomic approximation. [e] Ab initio dissociation energies. c = corrected for basis set superposition error, using the counterpoise correction. u = uncorrected for basis set superposition error. [f] References 2 or 7, except where stated otherwise. [g] Reference 26. [h] Reference 10. [i] Reference 27a. [j] Reference 27b. [k] Reference 28. Average values of D_e(Cu−Ng) are given. [l] Present work, unless otherwise indicated. [m] References 1 or 7, except where stated otherwise. [n] Reference 29. [o] Reference 30. [p] Reference 31. [q] Reference 6 or 7, except where stated otherwise. [r] Reference 5, except where stated otherwise. [s] Reference 7, unless otherwise stated. [t] Reference 8, unless otherwise indicated. [u] Reference 4, unless otherwise indicated. [v] Reference 32; apparent typographical error corrected. [w] Reference 3. [x] Reference 33. [y] Reference 34; σ_g and σ_u stretching frequencies are given, respectively. Dissociation energies given are one-half the atomization energies. [z] Reference 9. [aa] Reference 35.

Table 6. Comparison of Noble Gas−Noble Metal Bond Lengths (Å) in NgMX Complexes with Values Estimated from Standard Parameters

Standard Parameters			
atom/ion	van der Waals radius (r_{vdW})[a]	ionic radius (r_{ion})	covalent radius (r_{cov})
Ar	1.88		0.94−0.95[b] (0.98)[c]
Kr	2.00		1.09−1.11[b]
Xe	2.18		1.30−1.31[b]
Cu^+/Cu(I)		0.60[d]	1.06[e]
Ag^+/Ag(I)		0.81[d]	1.28[e]
Au^+/Au(I)		0.77[d]	1.27[e]
Na^+		0.79[d]	

Bond Lengths (r(Ng−M) in NgMX)				
	r_{vdW}(Ng) + r_{ion}(M^+)	experimental		r_{cov}(Ng) + r_{cov}(M(I))
ArCuX	2.48	2.22−2.30		2.04
KrCuX	2.60	2.32−2.3	...[f]	2.26
ArAgX	2.69	... 2.56−2.64		2.26
KrAgX	2.81	2.59−2.66		2.38
XeAgX	2.99	2.65−2.70	...	2.58
ArAuX	2.65	2.39−2.50		2.25
KrAuX	2.77	2.46−2.52	...	2.37
Ar−NaCl	2.67	2.89		

[a] Reference 36. [b] Reference 37. [c] Reference 38. [d] These are the values for coordination number 2. All are calculated from $r(M^+) = r(MF) - r(F^-)$. The values for Cu^+ and Ag^+ are from ref 39; those for Au^+ and Na^+ are newly calculated here. [e] Reference 40. [f] Dots show which sum of radii is closer to the experimental bond lengths.

The complexes in Table 6 are grouped according to the metal, with the experimental values presented between the sums in the van der Waals and covalent limits. In all cases, the experimental values are less than the van der Waals limit, and bigger than the covalent limit. (The exception is the undoubted van der Waals complex Ar−NaCl, in which the experimental value is greater than the van der Waals sum as defined here.) The dots (...) in Table 6 indicate where the experimental values are closer to one limit or the other. For NgAgX, which, from Table 5, are the most weakly bound of the noble metal complexes, there is a variation from Ng = Ar, where the experimental values are nearer the van der Waals limit, through Ng = Kr, where the differences are about equal, to Ng = Xe, where the experimental values are closer to the covalent limit. Where the metal is Cu or Au, however, the Ng = Ar complexes are intermediate between the two limits, and the Ng = Kr complexes are closer to the covalent side. One can anticipate from these trends that the Xe−Cu and Xe−Au bonds will be found to be very close to the covalent limit in XeCuX and XeAuX.

Vibration Frequencies and Dissociation Energies. Table 5 also contains a comparison of the centrifugal distortion constants of KrCuF and KrCuCl with those of the other NgMX complexes. The values for KrCuX are significantly less than those of the corresponding ArCuX complexes, mostly, but not entirely, because of the greater mass of Kr. The low values in all cases indicate that the complexes are rigid. They are much more rigid than the reference van der Waals complex Ar−NaCl, whose distortion constant is over an order of magnitude bigger.

The stretching frequencies ω(KrCu) were obtained from the distortion constants using the pseudo-diatomic equation:[41]

$$\omega(\mathrm{KrCu}) = \left(\frac{4B_o^3}{D_J}\right)^{1/2} \quad (4)$$

These results are also in Table 5 in comparison with ab initio values; the agreement between experiment and theory supports the use of eq 4 to derive the experimental values. From the comparison in Table 5, it is clear that the KrCuX complexes fit the established overall pattern: the ω(KrCu) frequencies are less than the corresponding ω(ArCu) values, very close to those of ω(KrAu), and considerably greater than the ω(KrAg) values. In all cases, these frequencies are much greater than the ω(ArNa) value for the Ar−NaCl van der Waals bond, and much nearer to low-end values for chemical bonds.

A better picture of the rigidity of the complexes has been obtained by evaluating the k(NgM) stretching force constants, thus removing any mass dependence from the measurements. Again, a pseudo-diatomic approximation was used, the results are in Table 5, and the present complexes are consistent with the other NgMX complexes. The k(KrCu) force constants are slightly bigger than the k(ArCu) constants, much greater than the corresponding k(KrAg) values, and somewhat less than the k(KrAu) values. They are 2 orders of magnitude greater than k(ArNa) in Ar−NaCl.

The last column of Table 5 gives ab initio NgM dissociation energies of all NgMX complexes reported to date, including KrCuF and KrCuCl. Three values are given for most complexes. Two are the results of MP2 calculations from the present work, in which basis set superposition error (BSSE) has and has not been accounted for. The third value is also an MP2 value, corrected for BSSE, from ref 10, obtained using a different program and basis set. There is general agreement between the two sets of values corrected for BSSE, with the possible exception of KrAgX values. The values calculated for KrCuF (45−48 kJ mol^{-1}) and KrCuCl (37−39 kJ mol^{-1}) approach the KrF bond energy in the compound KrF_2 (50 kJ mol^{-1}).[42]

(26) Hoeft, J.; Lovas, F. C.; Tiemann, E.; Törring, T. *Z. Naturforsch, A: Phys. Sci.* **1970**, *25*, 35.
(27) (a) Manson, E. L.; DeLucia, F. C.; Gordy, W. *J. Chem. Phys.* **1975**, *62*, 1040; (b) Manson, E. L.; DeLucia, F. C.; Gordy, W. *J. Chem. Phys.* **1975**, *63*, 2724.
(28) Bauschlicher, C. W., Jr.; Partridge, H.; Langhoff, S. R. *Chem. Phys. Lett.* **1990**, *165*, 272.
(29) Barrow, R. F.; Clements, R. M. *Proc. R. Soc. London, Ser. A* **1971**, *322*, 243.
(30) (a) Brice, B. A. *Phys. Rev.* **1931**, *35*, 960. (b) Pearson, E. F.; Gordy, W. *Phys. Rev., Ser. B* **1966**, *152*, 42.
(31) Brice, B. A. *Phys. Rev.* **1931**, *38*, 658.
(32) Andreev, S.; Bel Bruno, J. J. *Chem. Phys. Lett.* **2000**, *329*, 490.
(33) Evans, C. J.; Gerry, M. C. L. *J. Mol. Spectrosc.* **2000**, *203*, 105.
(34) Pyykkö, P. *J. Am. Chem. Soc.* **1995**, *117*, 2067.
(35) Ohshima, Y.; Iida, M.; Endo, Y. *J. Chem. Phys.* **1990**, *92*, 3990.
(36) Pyykkö, P. *Chem. Rev.* **1997**, *97*, 597.
(37) Bartlett, N.; Sladky, F. O. In *Comprehensive Inorganic Chemistry*; Bailar, J. C., Emeléus, H. J., Nyholm, R., Trotman-Dickenson, A. F., Eds.; Pergamon: Oxford, 1973; pp 213−330.
(38) Pyykkö, P. *Science* **2000**, *290*, 64.
(39) Huheey, J. E.; Keiter, E. A.; Keiter, R. L. *Inorganic Chemistry, Principles of Structure and Reactivity*, 4th ed.; Harper-Collins: New York, 1993.
(40) Pyykkö, P. *Chem. Rev.* **1988**, *88*, 579.
(41) Kratzer, A. *Z. Phys.* **1920**, *3*, 289.

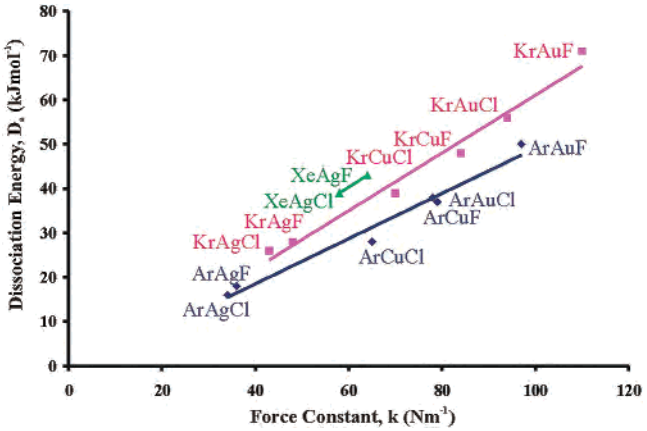

Figure 4. Plots of dissociation energy vs force constant for Ng−M bonds in NgMX complexes.

There is general correlation between the experimental force constants, k, and the ab initio dissociation energies, D_e. It is shown in Figure 4. This is approximately consistent with the Morse potential, for which k and D_e are related by:

$$k = 2D_e\beta^2 \qquad (5)$$

with β being the Morse potential constant. Thus, if the Morse potential holds and β is constant, then k and D_e are proportional. Figure 4 shows this to be roughly the case here. The centrifugal distortion constants, measured with the rotational spectrum, from which the force constants have been obtained, thus give an indirect, if approximate, measure of the Ng−M dissociation energies.

Since the ab initio D_e values are comparable to those of at least some clearly chemical bonds, it is appropriate to query whether such bonding is also found here. To test this idea, purely electrostatic induction energies have been calculated. In particular, given the linear NgMX geometry of the complexes, a good first approximation is the M^+−Ng charge-induced dipole term. Values calculated for this energy can be expected to be reduced by about 10% by the X^-−Ng term. The method of calculation is given in detail in ref 7.

Table 7 gives the induction energies for KrCuF and KrCuCl in comparison with those of the other NgMX complexes reported earlier.[7,10] Once again, the KrMX complexes fit well into the earlier picture: the calculated induction energies of the NgCuX and NgAgX complexes are $\sim 0.5D_e$, while those of the NgAuX are nearer to $0.1D_e$. For the accepted van der Waals complexes Ar−NaCl and Ar−BeO, the induction energies exceed D_e.

Several points must be considered in assessing these calculations. To start with, they assume a long-distance approximation, which may not be fully valid, and the calculated induction energies could be low by about 50%. If this were the case, they would barely exceed D_e for NgAgX, but would remain below D_e for NgCuX and far below D_e for NgAuX. Furthermore, although there are several other, smaller, attractive contributions to the induction energy, as well as dispersion terms which give contributions comparable to the charge-induced dipole term, they are counterbalanced by a significant repulsion energy.[12] Overall, it is not at all clear that the D_e values can be accounted for with purely electrostatic considerations. This is almost certainly not the case for NgAuX and also may well not be the case for NgCuX and NgAgX.

Table 7. Comparison of MX Dipole Moments and Effective Atomic Charges, Induction Energies, and ab Initio Dissociation Energies of NgMX Complexes

	MX			D_e[d]	
complex	μ[a]	q_{eff}[b]	$-E_{ind}$[c]	our work[e]	ref 10
ArCuF	5.77[f]	0.69	22	44[g]	37
ArCuCl	5.2[g]	0.53	13	33[g]	28
KrCuF	5.77[f]	0.69	28	45[h]	48
KrCuCl	5.2[g]	0.53	16	37[h]	39
ArAgF	6.22[f]	0.65	11	14[g]	18
ArAgCl	6.08[i]	0.55	8		16
KrAgF	6.22[f]	0.65	16	17[g]	28
KrAgCl	6.08[i]	0.55	11	15[g]	26
KrAgBr	5.62[j]	0.49	8	17[g]	
XeAgF	6.22[f]	0.65	24[j]	36[k]	43
XeAgCl	6.08[i]	0.55	16[j]	33[k]	39
ArAuF	3.4[g]	0.37	5	55[g]	50
ArAuCl	3.1[g]	0.29	3	42[g]	38
KrAuF	3.4[h]	0.37	6	58[g]	71
KrAuCl	3.1[g]	0.29	4	44[g]	56
Ar−NaCl	9.00[l]	0.79	10	8[m]	
Ar−BeO	7.2[n]	0.84	84	45[n]	

[a] μ is the dipole moment (Debye) of the MX monomer. [b] q_{eff} is the effective charge of the metal ion to produce the value of μ at the molecular bond length. It is in fractions of an elementary charge. Values from ref 7. [c] Charge-induced dipole induction energy (kJ mol^{-1}). [d] D_e in kJ mol^{-1}; BSSE is accounted for. [e] Values from ref 7 or 8, or present work. [f] Reference 26. [g] Reference 7. [h] Present work. [i] Reference 43. [j] Reference 44. [k] Reference 8. [l] References 45 and 46. [m] Reference 9. [n] Reference 47.

Nuclear Quadrupole Coupling Constants. In the present work, nuclear quadrupole coupling constants (NQCCs) have been evaluated for copper (^{63}Cu and ^{65}Cu), chlorine (^{35}Cl and ^{37}Cl), and ^{83}Kr. Each has provided useful information on the distribution of electron density at the nucleus in question.

The NQCCs for ^{63}Cu and ^{65}Cu, as well as for ^{35}Cl and ^{37}Cl, are in the ratios of their nuclear quadrupole moments (e.g., for ^{84}Kr^{63}CuF and ^{84}Kr^{65}CuF this ratio is 1.0805(8), very close to $eQ(^{63}Cu)/eQ(^{65}Cu) = 1.0806(3)$[48]). Accordingly, the discussion will consider only the ^{63}Cu and ^{35}Cl values.

Addition of the noble gases to CuX induces major changes to the $eQq(^{63}Cu)$ values. These are shown in Table 8. The NQCC of ArCuCl is roughly double that of CuCl, and that of KrCuCl is even bigger. However, those changes are better considered as additive rather than multiplicative. Thus, addition of Ar to CuX increases $eQq(^{63}Cu)$ by 16−17 MHz, while addition of Kr increases it by ∼20 MHz. The changes

(42) Lehmann, J. F.; Mercier, H. P. A.; Schrobilgen, G. J. *Coord. Chem. Rev.* **2002**, *233*−*234*, 1.
(43) Nair, K. P. R.; Hoeft, J. *J. Phys. B: At. Mol. Phys.* **1984**, *17*, 735.
(44) Nair, K. P. R.; Hoeft. J. *Chem. Phys. Lett.* **1982**, *102*, 438.
(45) Hebert, A. J.; Lovas, F. J.; Melendres, C. J.; Hollowell, C. D.; Story, T. L.; Street, K. *J. Chem. Phys.* **1968**, *48*, 2824.
(46) DeLeeuw, F. H.; Van Wachem, R.; Dymanus, A. *J. Chem. Phys.* **1969**, *50*, 1393.
(47) Veldkamp, A.; Frenking, G. *Chem. Phys. Lett.* **1994**, *226*, 11.
(48) Gordy, W.; Cook, R. L. *Microwave Molecular Spectra. No XVIII in Techniques of Chemistry*, 3rd ed.; Wiley: New York, 1984.

Table 8. ^{63}Cu Nuclear Quadrupole Coupling Constants (MHz) in ArCuX and KrCuX Complexes and Related Species

	$eQq(^{63}Cu)$		
molecule	X = F	X = Cl	X = Br
CuX	21.956[a]	16.16908[b]	12.8510[b]
ArCuX	38.056[a]	33.186[a]	29.92[c]
KrCuX	41.77[c]	36.52[c]	
$XCuX^-$		61.4[d]	57.7[e]
OCCuX	75.41[f]	70.83[f]	67.53[f]

[a] Reference 2. [b] Reference 49. [c] This work. [d] Reference 50. [e] Reference 51. [f] Reference 52.

Table 9. Halogen Quadrupole Coupling Constants (MHz) in CuCl, NgCuCl, and Related Species

parameter	CuX	ArCuX	KrCuX	$XCuX^-$	OCCuX
$eQq(^{35}Cl)$	−32.12729[a]	−28.032[b]	−27.30[c]	−19.3[d]	−21.474[e]
$eQq(^{79}Br)$	261.1799[a]	225.55[b]		152.8[f]	171.60[e]

[a] Reference 49. [b] Reference 2. [c] This work. [d] Reference 50. [e] Reference 52. [f] Reference 51.

are ∼38% and ∼45% of the change when X^- is added to form $XCuX^-$ ions. Similarly, addition of Ar and Kr causes changes of ∼30% and ∼37% of those obtained when CO is added to form the compounds OCCuX.[52] Clearly, very large redistributions of the electron density at Cu are obtained when the noble gases are added to CuX. Since both $XCuX^-$ and OCCuX are fully chemically bonded for all X, these results beg the question of whether the NgCuX complexes also show some degree of chemical bonding. It should be noted also that the fractional changes of the $eQq(^{63}Cu)$ are very close to those of $eQq(^{197}Au)$ on addition of Ng to AuX.[7] In the latter cases, the change in the NQCCs on addition of Ar or Kr to AuX are ∼33% and ∼42% of those found when X^- is added to form $XAuX^-$ ions and ∼27% and ∼35% of those found when CO is added to form OCAuX.

The ^{35}Cl and ^{79}Br nuclear quadrupole coupling constants are shown in Table 9. While their absolute changes on complex formation are less dramatic than those of the ^{63}Cu constants, their fractional changes are comparable. For example, the change on forming KrCuCl from CuCl is about 38% of the change on forming $ClCuCl^-$. This is comparable to, if a little smaller than, the fractional change in the ^{63}Cu constant (45%). This pattern is repeated for all ligands studied (Br, Cl, and CO).

The value of $eQq(^{83}Kr)$ in KrCuF is entirely in keeping with those of KrAgF and KrAuF. All three are given in Table 8, in comparison with those of several other Kr-containing complexes and of corresponding Xe-containing complexes. The NQCCs of both noble gases follow very similar trends; in particular, those of KrMX and XeMX are much larger than those of conventional van der Waals complexes, though well short of those of Kr^+ and of Xe ($[Kr]4d^{10}5p^5 6s^1$), respectively. Remarkably, $eQq(^{83}Kr)$ in KrCuF lies between the values for KrAgF and KrAuF. This is consistent with the trends found for the force constants and dissociation energies described above.

Table 10. ^{83}Kr and ^{131}Xe Nuclear Quadrupole Coupling Constants (MHz) for Various Kr- and Xe-Containing Species

molecule	$eQq(^{83}Kr)$	reference	molecule	$eQq(^{131}Xe)$	reference
Kr	0		Xe	0	
Kr−Ne	−0.52	54	Xe−Ne	0.39	55
Kr−Ar	−0.85	54	Xe−Ar	0.72	55
Kr−HCl	5.20	11	Xe−HCl	−4.9	56
KrCuF	128.79	this work			
KrAgF	105.10	6	XeAgF	−82.8	8
KrAuF	185.94	7	XeAgCl	−78.0	8
KrD^+	549	57	XeH^+	−369.5	58
Kr^+	915	59	$Xe([Kr]4d^{10}5p^5 6s^1)$	−505	60

Table 11. ^{83}Kr Nuclear Quadrupole Coupling Constants Resulting from Polarization Due to External Charges

					eQq (MHz)	
complex	q_{eff}[a]	E_{zz} (M)	E_{zz} (F)	E_{zz}[b]	calculated[c]	experimental
KrCuF	0.689	−1.593	0.294	−1.299	64	128.8
KrAgF	0.653	−1.069	0.195	−0.874	43	105.10
KrAuF	0.40	−0.715	0.127	−0.588	29	185.94
XeAgF	0.653	−0.994	0.189	−0.805	−34	−82.8
XeAgCl	0.555	−0.807	0.129	−0.678	−29	−78.2

[a] Fractional charge of the M^+ and F^- ions (Table 7). [b] E_{zz} is the sum of the field gradients at the Kr nucleus due to the M^+ and F^- ions alone (E_{zz}(M) and E_{zz}(F), respectively). Units are 10^{20} J C^{-1} m^{-2}. [c] Calculated using eqs 6 and 7 with $\gamma_\infty = 78$;[11] the second term of eq 6 is negligible.

As with the dissociation energies, it is also appropriate to consider whether the $eQq(^{83}Kr)$ values result simply from polarization of the spherical electron distribution of Kr by the external charges on MX, particularly CuX. The procedure for doing this was also described in ref 7. Basically this involves evaluating the field E_z and field gradient E_{zz} at the Kr nucleus due to MX alone, and then adjusting this value by adding in the polarized electrons. This is Sternheimer antishielding,[61,62] and the equations are:

$$V_{zz} = (\gamma^{Kr} + 1)E_{zz} + \epsilon^{Kr}E_z^{\,2} \quad (6)$$

$$eQq = -eQV_{zz} \quad (7)$$

Here γ^{Kr} and ϵ^{Kr} are Sternheimer shielding parameters (=78 and 5 V^{-1} respectively for ^{83}Kr). As was found earlier,[7] the term $\epsilon^{Kr}E_z^{\,2}$ is negligible. The values for ^{83}KrCuF are given in Table 11, in comparison with those of the other reported complexes. Again, the calculated eQq falls far short of the

(49) Low, R. J.; Varberg, T. D.; Connelly, J. P.; Auty, A. R.; Howard, B. J.; Brown, J. M. *J. Mol. Spectrosc.* **1993**, *161*, 499.
(50) Bowmaker, G. A.; Brockliss, L. D.; Whiting, R. *Aust. J. Chem.* **1973**, *26*, 29.
(51) Bowmaker, G. A.; Boyd, P. D. W.; Sorrensen, R. J. *J. Chem. Soc., Faraday Trans. 2* **1985**, *81*, 1627.
(52) Walker, N. R.; Gerry, M. C. L. *Inorg. Chem.* **2001**, *40*, 6158.
(53) Evans, C. J.; Reynard, L. M.; Gerry, M. C. L. *Inorg. Chem.* **2001**, *40*, 6123.
(54) Xu, Y.; Jäger, W.; Djauhari, J.; Gerry, M. C. L. *J. Chem. Phys.* **1995**, *103*, 2827.
(55) Xu, Y.; Jäger, W.; Gerry, M. C. L. *J. Chem. Phys.* **1993**, *99*, 919.
(56) Keenan, M. R.; Buxton, L. W.; Campbell, E. J.; Balle, T. J.; Flygare, W. H. *J. Chem. Phys.* **1980**, *73*, 3523.
(57) Warner, H. E.; Conner, W. T.; Woods, R. C. *J. Chem. Phys.* **1984**, *81*, 5413.
(58) Peterson, K. A.; Petrmichl, R. H.; McClain, R. L.; Woods, R. C. *J. Chem. Phys.* **1991**, *95*, 2352.
(59) Holloway, J. H.; Schrobilgen, G. J.; Bukshpan, S.; Hilbrants, W.; deWaard, H. *J. Chem. Phys.* **1977**, *66*, 2627.
(60) Faust, W. L.; McDermott, M. N. *Phys. Rev.* **1961**, *123*, 198.
(61) Foley, H. M.; Sternheimer, R. M.; Tycko, D. *Phys. Rev.* **1954**, *93*, 734 and references therein.
(62) (a) Fowler, P. W.; Lazzeretti, P.; Steiner, E.; Zanasi, R. *Chem. Phys.* **1989**, *133*, 121. (b) Fowler, P. W. *Chem. Phys. Lett.* **1989**, *156*, 494.

Table 12. Comparison of ^{79}Br and ^{83}Kr Nuclear Quadrupole Coupling Constants (eQq_o) and Field Gradients (q_o)

	^{79}Br		^{83}Kr	
molecules	eQq_o (MHz)	q_o[a]	eQq_o (MHz)	q_o[a]
DBr/DKr$^+$	530.648[b]	16.95	549.1[c]	21.20
BrCuBr$^-$/KrCuF	152.8[d]	4.88	128.79	4.97
BrAuBr$^-$/KrAuF	202.3[d]	6.45	185.9[e]	7.18
OCCuBr/KrCuF	171.6[f]	5.48	128.79	4.97
OCAgBr/KrAgF	223.9[g]	7.15	105.1	4.06
OCAuBr/KrAuF	285.1[h]	9.11	185.9[e]	7.18

[a] *Relative* values ($\equiv eQq_o/eQ$ in MHz fm^{-2}), calculated using $eQ(^{79}\text{Br}) = 31.3$ fm^2 (ref 63) and eQ (^{83}Kr) = 25.9 fm^2 (ref 64). [b] Reference 65. [c] Reference 57. [d] Reference 51. [e] Reference 7. [f] Reference 52. [g] Reference 66. [h] Reference 53.

experimental value, and an alternative mechanism to electrostatic polarization must be sought to rationalize the coupling constants.

A different view presented earlier[7] also applies to ^{83}Kr^{63}Cu^{19}F. Because Br is adjacent to Kr in the periodic table, it is appropriate to compare field gradients at Br and Kr in isoelectronic ions and molecules. Such a comparison is in Table 12. It is interesting that in each of the pairs DBr/DKr$^+$, BrAuBr$^-$/KrAuF, and BrCuBr$^-$/KrCuF the field gradient at Kr is very similar to that at Br. The inference is that the electron distributions at Br and Kr are very similar within each pair of complexes. A similar consideration applies to the comparison with the carbonyl complexes, whose values are also in Table 12.

The $eQq(^{83}\text{Kr})$ value can also give a simple indication of the charge displaced from Kr to CuF. Complete removal of an electron would give Kr$^+$, for which $eQq(^{83}\text{Kr}) = 915$ MHz. Thus, the degree of charge displacement from Kr is $129/915 = 0.14$ of an electron. This should be contrasted with 0.006 of an electron in Kr−HCl.

Electron Distributions from ab Initio Calculations. Along with the bond lengths, vibration frequencies, and NgM dissociation energies, the ab initio calculations produced information on the electron distribution of the complexes. In particular, Mulliken populations, as well as MOLDEN plots of electron density of valence molecular orbitals and Laplace concentrations, have been obtained. In addition, electron localization functions (ELFs) have been calculated.

The Mulliken populations are shown in Table 13. For both complexes, the most striking results are changes in the 4s and 4p populations on Kr. For both complexes, there is apparently a σ-donation of 0.13−0.14 electron from Kr to CuX, with a marginal π-donation (if any). Most of this is taken up by the 4sσ orbitals on Cu, with rather less to 4pσ. Interestingly, there is also a small *decrease* in the 3dσ populations on Cu.

Figure 5 shows MOLDEN plots of contours of electron density of fully occupied 3σ- and 1π-valence MOs for KrCuF. For all four orbitals, the plots suggest significant sharing of electron density between 4p orbitals on Kr and 3d orbitals on Cu. The σ-sharing is greater than the π-sharing. Such sharing would appear to be a requirement if there is to be chemical bonding. It is interesting that we have *not* been able to construct corresponding MOs with comparable

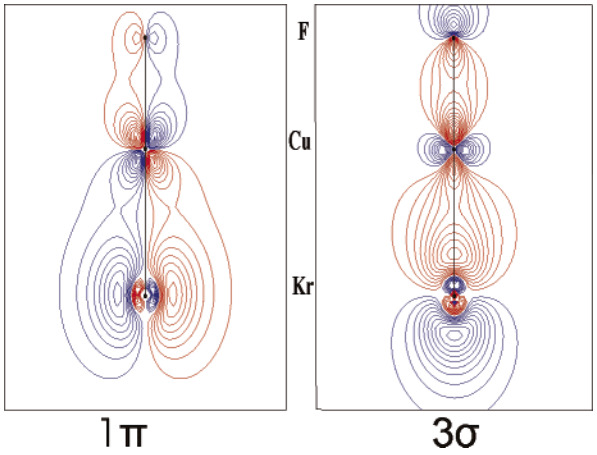

Figure 5. MOLDEN contour diagrams of two occupied valence molecular orbitals of KrCuF; in each case, the value of the contours is $n = 0.02$ with $n = 1-13$. The different colors indicate opposite signs of the wave function.

Table 13. Mulliken Valence Orbital Populations (n) for Kr, CuF, KrCuF, CuCl, and KrCuCl

orbital population	Kr + CuF	KrCuF	Kr + CuCl	KrCuCl
	Kr		Kr	
q	0	0.13	0	0.13
n_s	2.00	1.99	2.00	1.98
$n_{p\sigma}$	2.00	1.88	2.00	1.88
$n_{p\pi}$	4.00	3.98	4.00	3.98
$n_{d\sigma}$	2.00	2.00	2.00	2.00
$n_{d\pi}$	4.00	4.00	4.00	4.01
$n_{d\delta}$	4.00	4.00	4.00	4.00
	Cu		Cu	
q	0.64	0.50	0.49	0.37
n_s	0.23	0.34	0.32	0.39
$n_{p\sigma}$	0.05	0.09	0.12	0.18
$n_{p\pi}$	0.12	0.11	0.10	0.09
$n_{d\sigma}$	1.93	1.89	1.96	1.93
$n_{d\pi}$	4.06	4.06	4.04	4.03
$n_{d\delta}$	4.00	4.00	4.00	4.00
	F		Cl	
q	−0.64	−0.63	−0.49	−0.51
n_s	2.00	1.99	2.01	1.97
$n_{p\sigma}$	1.81	1.80	1.68	1.66
$n_{p\pi}$	3.84	3.83	3.93	3.87

sharing for either of the accepted van der Waals complexes Ar−NaCl and Ar−BeO.

Plots of Laplace concentrations, $-\nabla^2\rho(r)$, for both complexes are in Figure 6. These plots show where the total electron density of the molecule concentrates and provide another approach to discussing chemical bonding. In the case of NgBeO, distortion of the Laplace concentrations was deemed to indicate the degree of covalency of the Ng−Be bond:[67] a clear lobe for Xe was taken to indicate the onset of covalent bonding.[68] For KrCuF and KrCuCl, such distortion is slight (Figure 6), so by this criterion, the bonding is considered largely electrostatic.

(63) Pyykkö, P. *Mol. Phys.* **2001**, *99*, 1617.
(64) Kellö, V.; Pyykkö, P.; Sadlej, A. J. *Chem. Phys. Lett.* **2001**, *346*, 155.
(65) DeLucia, F. C.; Helminger, P.; Gordy, W. *Phys. Rev. A: At., Mol., Opt. Phys.* **1971**, *3*, 1849.
(66) Walker, N. R.; Gerry, M. C. L. *Inorg. Chem.* **2002**, *41*, 1236.
(67) Frenking, G.; Koch, W.; Gauss, J.; Cremer, D. *J. Am. Chem. Soc.* **1988**, *110*, 8007.
(68) Veldkamp, A.; Frenking, G. *Chem. Phys. Lett.* **1994**, *226*, 11.

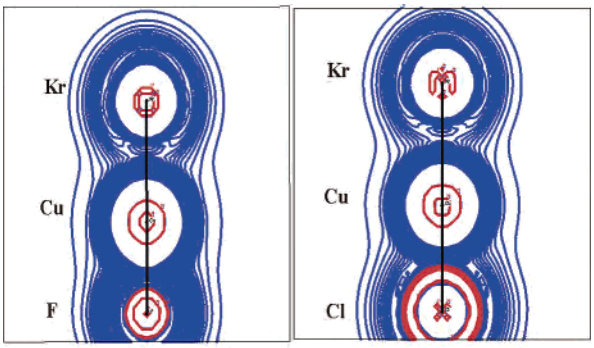

Figure 6. MOLDEN contour plots of the Laplace concentrations of the electron density for (a) KrCuF and (b) KrCuCl. Blue and red indicate positive and negative values of $-\nabla^2\rho(r)$, respectively.

As an alternative to the use of the Laplace concentration, a topological analysis of the ELF has been carried out. This function, $\eta(x,y,z)$, is defined by:[69−72]

$$\eta(x,y,z) = \left(1 + \left(\frac{D_\sigma(x,y,z)}{D_\sigma^0(x,y,z)}\right)^2\right)^{-1} \quad (8)$$

where D_σ and D_σ^0 represent the curvature of the electron pair density of electrons of identical spin, σ, for the actual system (D_σ) and for a homogeneous electron gas of the same density (D_σ^0). The original interpretation[69] was that where $D_\sigma = 0$, making $\eta = 1$, there is zero probability of finding electrons of the same spin, but that electron pairs of opposite spin can congregate. Where $D_\sigma = D_\sigma^0$, making $\eta = 0.5$, there is perfect delocalization, and where $\eta < 0.5$, there is very little electron density. More recently, it was shown that $\eta < 0.5$ can also occur where there are many nodes in the spatial wave functions, and significant electron density can be masked.[71]

Savin et al.[70] have put forward an interpretation of the topology of the ELF for a given molecule in which topological domains are located and assigned chemical significance. This type of analysis, when applied to the results of the KrCuF ab initio calculations described above, demonstrates the presence of a so-called "disynaptic-valence attractor", V(Kr,Cu), located between, and associated with, the Kr and Cu core basins. Savin et al. characterize di- or polysynaptic attractors of this type as a shared-electron interaction and thus, presumably, a covalent bond. For KrCuF, the analysis demonstrates that the electron population of V(Kr,Cu) is small, and this suggests that the covalent interaction between the Kr and Cu centers is very weak.

Concluding Remarks

The complexes KrCuF and KrCuCl have been detected and characterized using Fourier transform microwave rotational spectroscopy. Rotational constants and centrifugal distortion constants have been precisely evaluated and have produced geometries and vibrational data. These results have been confirmed with ab initio calculations. Nuclear quadrupole coupling constants (NQCCs) for ^{83}Kr, Cu, and Cl have also been evaluated. Kr−CuX dissociation energies, D_e, have been calculated ab initio, along with various indicators of electron distribution.

Both KrCuF and KrCuCl fit the trends established for other noble gas−noble metal halide (NgMX) complexes studied to date. The Kr−Cu bonds are short and the complexes are rigid. The Kr−Cu stretching force constants, k, are larger than the Ar−Cu values. Their values follow the trend k(KrAg) < k(KrCu) < k(KrAu), a trend paralleled by the dissociation energies. It is also paralleled by the ^{83}Kr NQCCs, which are large. The NQCC for KrCuF is greater than that for KrAgF but less than that for KrAuF, showing that the distortion of the noble gas electron distribution on complex formation follows the trend Ag < Cu < Au. All three parameters (force constants, dissociation energies, and nuclear quadrupole coupling constants) imply that the Ng−M bonds are rather stronger than simple van der Waals bonds.

Though KrCuF and KrCuCl are consistent with other known NgMX complexes, they have done little to resolve the puzzle of the nature of the Ng−M bonds. Thus, Ng−M^+ induction energies are $\sim 0.5D_e$ for all NgCuX and NgAgX, but $\sim 0.1D_e$ for NgAuX. The Ng−M bonds are significantly shorter than corresponding sums of Ng van der Waals radii and M^+ ionic radii and are, if anything, closer to the sums of the Ng and M(I) covalent radii. The NQCCs of all atoms indicate significant reorganization of electron distribution on complex formation. The values for ^{83}Kr (or ^{131}Xe)[8] could not be accounted for with a simple electrostatic model. The field gradient at Kr in KrCuF is close to that at Br in isoelectronic $BrCuBr^-$, also consistent with related complexes. The eQq(^{83}Kr) value suggests a donation of 0.14 electron from Kr to CuF, a value which is confirmed by ab initio Mulliken populations. MOLDEN plots of occupied valence molecular orbitals continue to imply significant sharing between Ng and MX (which we could not show for Ar−NaCl or Ng−BeO van der Waals complexes). On the other hand, MOLDEN plots of Laplace concentrations and ELF calculations indicate only small electron buildup between the Ng and M nuclei.

It is clear that, overall, the NgMX complexes are at the border between van der Waals and chemical bonding. van der Waals bonding can account for most of the properties of NgAgX but is entirely inadequate to deal with NgAuX. The NgCuX are intermediate, with KrCuF and KrCuCl perhaps closest of all to the border. Making the distinction is hampered by the lack of a clear definition of a chemical bond and of a clear criterion for such bonding. (A recent exchange in the literature illustrates the dilemma.[73,74]) None of the experimental parameters can be fully accounted for with a model in which the noble gas and metal halide are simply resting against each other, and further rationales must be sought.

(69) Becke, A. D.; Edgecombe, K. E. *J. Chem. Phys.* **1990**, *92*, 5397.
(70) Savin, A.; Silvi, B.; Colonna, F. *Can. J. Chem.* **1996**, *74*, 1088.
(71) Burdett, J. K.; McCormick, T. A. *J. Phys. Chem. A* **1998**, *102*, 6366.
(72) Berski, S.; Latajka, Z.; Andrés, J. *Chem. Phys. Lett.* **2002**, *356*, 483.
(73) Frenking, G. *Angew Chem., Int. Ed.* **2003**, *42*, 143; **2003**, *42*, 3335.
(74) Gillespie, R.; Popelier, P. L. A. *Angew. Chem., Int. Ed.* **2003**, *42*, 3331.

Table 14. Changes in Mulliken Populations on Complex Formation

	Ng		M		
	Δn_s	$\Delta n_{p\sigma}$	Δn_s	$\Delta n_{p\sigma}$	$\Delta n_{d\sigma}$
ArCuF	0	−0.08	0.12	0.02	−0.05
ArCuCl	0	−0.08	0.07	0.04	−0.04
ArCuBr	0	−0.08	0.08	0.04	−0.02
KrCuF	−0.01	−0.12	0.12	0.04	−0.04
KrCuCl	−0.02	−0.12	0.09	0.07	−0.03
ArAgF	0	−0.04	0.07	0	−0.02
ArAgCl	0	−0.04	0.05	−0.01	−0.02
ArAgBr	0	−0.04	0.03	−0.01	−0.01
KrAgF	0	−0.07	0.09	0.01	−0.03
KrAgCl	0	−0.06	0.08	−0.01	−0.03
KrAgBr	0	−0.06	0.05	−0.01	−0.02
XeAgF	0	−0.04	0.07	0	−0.04
XeAgCl	0	−0.04	0.10	−0.03	−0.04
ArAuF	0	−0.12	0.18	0.05	−0.09
ArAuCl	−0.02	−0.12	0.13	0.04	−0.05
ArAuBr	−0.02	−0.11	0.17	0.05	−0.04
KrAuF	−0.02	−0.19	0.22	0.07	−0.09
KrAuCl	−0.03	−0.17	0.17	0.07	−0.06

It is particularly interesting that, for a given Ng, all indicators of bond strength follow the trend Ag < Cu < Au. This applies not only to the properties mentioned above but also to the changes in Mulliken populations on complex formation; our values are in Table 14. Donations are, for Ar and Kr, ∼0.06 e^- for Ng−Ag, 0.1 e^- for Ng−Cu, and 0.15 e^- for Ng−Au.

One property common to the noble metals but not to Na or Be is the availability of low-lying d orbitals for bonding. If the bonding is thought of as involving some sd hybrid orbitals on the metal, then an important property is the energy required to excite an nd electron on M to (n +1)s. For M^+, these follow the trend Ag^+ (39164 cm^{-1}) > Cu^+ (21928 cm^{-1}) > Au^+ (15039 cm^{-1})![75] So sd hybridization is much more difficult for Ag than for Cu or Au, in keeping with the trends for the NgMX complexes. It is amusing to note that changes in nd Mulliken populations on complex formation (Table 14, column 7) follow roughly the same trend.

If the d orbitals on M are essential in the Ng−M bonds (and all evidence, particularly the MOLDEN plots of the valence MOs, suggests that they are), then it must be argued that these bonds *all* show a greater or lesser degree of chemical bonding for *all* the complexes. For our purposes, we will regard a chemical bond as occurring between two atoms when electron density on one atom when they are not bonded can have a significant probability of being in the sphere of influence (orbitals?) of the other atom when they are bonded. Both the Laplace concentrations and ELFs give only a weak indication of covalent bonding, implying the bonding to be electrostatic. This could be interpreted as polarization/dispersion van der Waals bonding. However, for KrCuX, as with XeAgX and $AuXe_4^{2+}$, the noble gas NQCCs and/or the Mulliken populations indicate a small charge displacement from Ng to M, thus suggesting weak chemical bonding.

Acknowledgment. This research has been supported by the Natural Sciences and Engineering Research Council of Canada.

Supporting Information Available: Measured transition frequencies with their quantum number assignments. This material is available free of charge via the Internet at http://pubs.acs.org.

IC040009S

(75) Moore, C. E. *Atomic Energy Levels*, NBS Circular 467, 1958.